Modification of the Elastic Constants of a Peptide-Decorated Lamellar Phase

Nicolas Tsapis,*,† Raymond Ober,‡ Alain Chaffotte,§ Dror E. Warschawski,|| John Everett,⊥ John Kauffman,⊥ Peter Kahn,⊥ Marcel Waks,# and Wladimir Urbach†

Laboratoire de Physique Statistique de l'Ecole Normale Supérieure, UMR 8550 CNRS, 24 rue Lhomond, 75231 Paris Cedex 05, France, Laboratoire de Physique de la Matière Condensée, Collège de France and URA 792 CNRS, 5 Place Marcellin Berthelot, 75231 Paris Cedex 05, France, Biochimie Cellulaire, Dept B.G.M., Institut Pasteur, 28, rue du Dr. Roux, 75724 Paris Cedex 15, France, UMR 7099 CNRS, IBPC, 13 rue P. et M. Curie, 75005 Paris, France, Department of Biochemistry and Microbiology, Rutgers University, 76 Lipman Drive, New Brunswick, New Jersey 08901, and Laboratoire d'Imagerie Paramétrique, UMR 7623 CNRS, 15 rue de l'Ecole de Médecine, 75270 Paris Cedex 06, France

Received December 18, 2001. In Final Form: March 28, 2002

We have investigated the effect of the insertion of a triblock peptide (hydrophobic−hydrophilic−hydrophobic) in a nonionic lamellar phase composed of $C_{12}E_4$, decane, and water, stabilized by bilayer thermal fluctuations. Circular dichroism shows the peptide to be unordered in water, whereas its hydrophilic part is rigid and organized in an α-helix in the presence of surfactant bilayers. Surface tension measurements prove that the peptide is located at the hydrophobic−hydrophilic interface. Together with spectrofluorometry, these experiments suggest that the peptide lies on the bilayer surface. The Caillé parameter, η, of the lamellar phase, obtained by SAXS experiments, decreases with peptide concentration. This decrease has been interpreted as an increase of the bilayer effective thickness induced by the peptide and is well fitted by a recent model. The bilayer bending rigidity κ increases linearly with peptide concentration, up to two times the rigidity of a bare bilayer with mole ratio of peptide to surfactant as low as 5.2×10^{-4}. The smectic compressibility modulus, $\bar{B}$, decreases, implying that the peptide presence softens interactions between bilayers.

1. Introduction

Mesophases of surfactants containing host macromolecules have attracted a great deal of attention during the past decade because of their industrial interest as well as the theoretical problems they raise. Studies of the influence of polymers on the elastic properties of bilayers are relevant, for example, to drug delivery by vesicles. These drugs exist in solution, adsorbed on the membrane of a vesicle, or can protrude into the membrane itself. Several theoretical studies have been directed toward the effect of flexible polymers (adsorbed[1−3] or end-grafted[4−9]) on the elastic properties of lamellar phases. Many experiments have been performed, incorporating long flexible polymers in a lamellar (L_α) phase.[10−20] There are only a few experimental reports on the variations of the bilayer bending rigidity, κ, or the smectic compressibility modulus, $\bar{B}$, induced by addition of flexible polymers.[16−20]

The effect of rigid inclusions on the bending rigidity has been theoretically studied, however, for an isolated bilayer/membrane[21] or for a lamellar phase.[22,23] To the best of our knowledge, very few experiments have been performed with rigid inclusions.[24] Yet, a rigid peptide can be considered as a more realistic object to mimic proteic/peptidic drugs in vesicles than flexible polymers. Another

* To whom correspondence should be addressed. E-mail: ntsapis@deas.harvard.edu. Current address: DEAS, Harvard University, 9 Oxford St., Cambridge, MA 02138.

† Laboratoire de Physique Statistique de l'Ecole Normale Supérieure, UMR 8550 CNRS.

‡ Laboratoire de Physique de la Matière Condensée, Collège de France and URA 792 CNRS.

§ Institut Pasteur.

|| UMR 7099 CNRS, IBPC.

⊥ Rutgers University.

Laboratoire d'Imagerie Paramétrique, UMR 7623 CNRS.

(1) De Gennes, P.-G. *J. Phys. Chem.* **1990**, *94*, 8407.

(2) Brooks, J. T.; Marques, C. M.; Cates, M. E. *Europhys. Lett.* **1991**, *14*, 713. Brooks, J. T.; Marques, C. M.; Cates, M. E. *J. Phys. II* **1991**, *6*, 673.

(3) Clément, F.; Joanny, J. F. *J. Phys. II* **1991**, *7*, 973.

(4) Cantor, R. *Macromolecules* **1981**, *14*, 1186.

(5) Milner, S. T.; Witten, T. A.; Cates, M. E. *Macromolecules* **1989**, *22*, 853.

(6) Lipowsky, R. *Europhys. Lett.* **1995**, *30*, 197.

(7) Hiergeist, C.; Lipowsky, R. *J. Phys. II* **1996**, *6*, 1465.

(8) Marques, C. M.; Fournier, J. B. *Europhys. Lett.* **1996**, *35*, 361.

(9) Porte, G.; Ligoure, C. *J. Chem. Phys.* **1995**, *102*, 4290.

(10) Iliopoulos, I.; Olsson, U. *J. Phys. Chem.* **1994**, *98*, 1500.

(11) Kékicheff, P.; Cabane, B.; Rawiso, M. *J. Colloid Interface Sci.* **1984**, *120*, 51.

(12) Ligoure, C.; Bouglet, G.; Porte, G. *Phys. Rev. Lett.* **1993**, *71*, 3600.

(13) Ficheux, M.-F.; Bellocq, A.-M.; Nallet, F. *J. Phys. II* **1995**, *823*, 5.

(14) Radlinska, E. Z.; Gulik-Krzywicki, T.; Lafuma, F.; Langevin, D.; Urbach, W.; Williams, C. E. *J. Phys. II* **1997**, *7*, 1393.

(15) Warriner, H.; Idziak, S. H. J.; Slack, N. L.; Davidson, P.; Safinya, C. R. *Science* **1996**, *271*, 969.

(16) Porcar, L.; Ligoure, C.; Marignan, J. *J. Phys. II* **1997**, *7*, 1.

(17) Bouglet, G.; Ligoure, C. *Eur. Phys. J. B* **1999**, *9*, 137.

(18) Warriner, H. E.; Keller, S. L.; Idziak, S. H. J.; Slack, N. L.; Davidson, P.; Zasadzinski, J. A.; Safinya, C. R. *Biophys. J.* **1998**, *75*, 272.

(19) Castro-Roman, F.; Porte, G.; Ligoure, C. *Phys. Rev. Lett.* **1999**, *82*, 109.

(20) Yang, Y.; Prudhomme, R.; McGrath, K. M.; Richetti, P.; Marques, C. M. *Phys. Rev. Lett.* **1998**, *80*, 2729.

(21) Netz, R. R.; Pincus, P. *Phys. Rev. E* **1995**, *52*, 4114.

(22) Chen, C.-M. *Physica A* **2000**, *281*, 41.

(23) Sens, P.; Turner, M. S. *Eur. Phys. J. E* **2001**, *4*, 115−120.

(24) Taulier, N.; Nicot, C.; Waks, M.; Hodges, R. S.; Ober, R.; Urbach, W. *Biophys. J.* **2000**, *78*, 857.

10.1021/la015745c CCC: $22.00
Published on Web 05/02/2002

interesting feature of peptides is the high reproducibility of their synthesis and their monodispersity compared to that for polymers. Moreover peptides have a higher biological relevance than polymers because of the secondary structure they can adopt (α-helices, β-sheets).

In the present article, we report the extent to which the insertion of a rigid triblock peptide affects the elastic properties of an L_α phase stabilized by thermal fluctuations. Nonionic surfactant bilayers have been chosen as an appropriate model for the study of the peptide insertion into bilayers in the absence of long-range electrostatic interactions. The ternary system tetraethylene glycol monododecyl ether (denoted $C_{12}E_4$), water, and decane, which displays stable L_α and spongelike phases (L_3) between 20 and 30 °C, has been selected. In such systems (L_α or L_3), two monolayers of surfactant enclosing decane will be called a bilayer hereafter. The lamellar system is made of stacks of such bilayers periodically separated by water, whereas the L_3 phase consists of a multiconnected bilayer separating water into two distinct spaces. Locally however, the structure is the same as that in a lamellar phase: a bilayer surrounded by water. Since the L_3 phase is optically isotropic, circular dichroism, ultraviolet (UV) spectroscopy, and spectrofluorometry experiments can be carried out on this phase.

The sequence of the peptide has been designed in order to obtain two hydrophobic tails and a hydrophilic rigid core organized into an α-helix. Its structure has been examined by circular dichroism (CD). Changes induced by addition of the peptide to the lamellar phase have been determined by small-angle X-ray scattering (SAXS). In particular, the effects of the peptide concentration on the Caillé parameter, η, the bilayer bending rigidity, κ, and the smectic compressibility modulus, B, have been examined and compared to theoretical predictions.[21−23]

2. Materials and Methods

2.1. Materials. *2.1.1. Solvents and Surfactants.* Decane was purchased from Sigma (purity > 99%). Perdeuterated decane (purity > 99%) was purchased from Eurisotop (France). The nonionic surfactant NIKKOL BS-4LY tetraethylene glycol monododecyl ether (denoted $C_{12}E_4$) was obtained from Nikko Chemicals Co. Ltd. (Japan) at a purity = 99%. These products were used without further purification. Water was purified with a Milli-Q system from Millipore. Because of the very small amount of peptide solubilized in water, the density of the solution (1 g/mL) has been considered unchanged. The surfactant density has been measured equal to 0.942 g/mL for $C_{12}E_4$,[25] and the decane density was taken equal to 0.73 g/mL.

2.1.2. Peptide. The peptide, of length 30 residues, was designed to have a hydrophilic center region of 15 residues flanked by hydrophobic sequences of six residues at the amino end and nine on its carboxyl side. The molecular weight of the peptide is 3508.7. Its sequence is shown below:

```
Ala Ser Pro Ala Leu Trp
 1               5
Lys Lys Gln Glu Gln Glu Gln Gln Gln Glu Gln Glu Gln Lys Lys
 7              10                  15                  20
Trp Leu Leu Val Ile Gly Ser Gly Leu
22              26
```

In the physiological pH range, the hydrophilic part has no net charge, although it contains a number of charged amino acid side chains, and the peptide as a whole is globally neutral, as well. Its predicted pI (isoelectric point) is 6.33. Since we worked in pure water, the peptide is considered globally neutral. The hydrophilic region has two lysine residues at each end. The rest of the hydrophilic part consists solely of glutamic acid and glutamine residues. Enrichment of the hydrophilic region with charged groups helps ensure aqueous solubility despite the hydrophobic ends. The glutamate and glutamine residues are arranged in a mirror repeat: NENENNNENEN. This patterning allows their side chains to form Glu−Gln hydrogen bonds, supplementing the hydrogen bonds of the α-helix in this region. When the peptide is modeled and its energy minimized, four such hydrogen bonds form with standard geometry: Gln9−Glu12, Glu10−Gln13, Gln15−Glu18, and Glu16−Gln19. Lys−Glu interactions are also possible, although some of the side-chain-to-side-chain hydrogen bonds may be replaced by side-chain-to-membrane and peptide-to-water H-bonds in the lamellar phase.

Working outward from the hydrophilic center, the hydrophobic regions each begin with a tryptophan (Trp) residue to make possible concentration determination by UV absorbance. Next comes a leucine to increase the hydrophobicity. The remainders of the flanking regions are helix-capping motifs,[26] which would serve to reduce the helix dipole.

The rise per residue of an α-helix is 0.15 nm. If all 30 residues were to be helical, the peptide's length would be 4.5 nm.

Molecular modeling and minimization of conformational energy were performed with the Insight II program (Molecular Simulations, Inc., San Diego, CA). Energy minimization was used to ensure the absence of steric overlaps and to verify that the hydrogen bonds and other interactions could occur with standard geometries.

2.1.3. Sample Preparation. Stock solutions of surfactant and decane at constant volume ratio $V_s/(V_s + V_{decane}) = 0.55$, where V_s is the volume of surfactant, were prepared by weighing components and mixing them together. This process allows one to minimize concentration errors and to work at the same bilayer thickness (5.6 nm here[25]). The peptide was dissolved in water, and its concentration was measured by UV absorption spectroscopy, since it has two tryptophans in its sequence. Ingredients were then mixed, keeping the bilayer volume fraction constant $\phi = (V_s + V_{decane})/(V_s + V_{decane} + V_{aq}) = 0.38$, where V_{aq} is the volume of aqueous solution, and centrifuged at 5000 rpm for 10 min. The parameter R is defined as the mole ratio of peptide-to-surfactant: $R \equiv$ [peptide]/[surfactant]. To estimate the bilayer bending rigidity at 20 °C, lamellar phases at constant R and volume ratio $V_s/(V_s + V_{decane}) = 0.55$ have been studied by varying the bilayer volume fraction between 0.38 and 0.52. This rather small range of bilayer volume fraction is due to the phase boundaries: below $\phi \approx 0.35$, a lamellar phase in coexistence with an isotropic phase has been observed. For bilayer volume fraction above 0.35, samples are monophasic and in the lamellar phase.

2.2. UV Absorption Spectroscopy. UV spectroscopy was performed on a Beckman DU 7400 spectrophotometer. The background spectrum of the peptide-free sample (water or sponge phase) was measured and subtracted from the peptide-containing sample signal. Samples were maintained at the desired temperature (20 °C for the peptide solution and 28 °C for the sponge phase) using a thermostated bath, regulated within ±0.1 °C. The extinction coefficient of tryptophan, 5500 $M^{-1}\cdot cm^{-1}$ at 280 nm,[27] was used as the basis of the peptide extinction coefficient (11 000 $M^{-1}\cdot cm^{-1}$).

2.3. Surface Tension Measurements. Surface tension measurements were performed using the drop weight technique at the water−decane interface.[28] Pure water and a 0.105 mg/mL peptide solution were used. The syringe piston was pushed at the speed 1 mm/min. The needle radius is 0.75 mm. The Harkins and Brown correction factor was taken into account in the drop weight calculations, as was decane evaporation.

2.4. Circular Dichroism. Circular dichroism (CD) measurements were performed on a CD6 Jobin-Yvon (France) spectropo-

(25) Tsapis, N.; Ober, R.; Urbach, W. *Langmuir* **2000**, *16*, 2968.

(26) Aurora, R.; Rose, G. D. *Protein Sci.* **1998**, *7*, 21.

(27) Greenstein, J. P.; Winitz, M. *Chemistry of the amino acids*; John Wiley and Sons: New York, 1961.

(28) Middleman, S. *Modelling axisymmetric flows*; Academic Press: San Diego, 1995; Chapters 4 and 6. Lord, R. Investigations in capillarity. *Philos. Mag.* **1899**, *48*, 321. Harkins, W. D.; Brown, F. E. *J. Am. Chem. Soc.* **1919**, *41*, 499. Garandet, J. P.; Vinet, B.; Gros, P. *J. Colloid Interface Sci.* **1994**, *165*, 351.

larimeter. The temperature of the sample was regulated with an accuracy of ±0.1 °C. Measurements in the far UV (200−260 nm) were achieved at 28 °C, on an aqueous solution of peptide and on an isotropic sponge phase containing peptide. Samples were measured in a 0.2 mm path Hellma cuvette and scanned in 0.5 nm steps. The background spectrum of the peptide-free samples (water or sponge phase) was subtracted from the peptide-containing sample signal. Scans were run five times and averaged. The results are expressed as mean residue ellipticity $[\theta]$ (in deg·cm^2·dmol^{-1}):

$$[\theta] = \frac{M}{n}\frac{3300\Delta A}{Lc} \tag{1}$$

where M is the molecular weight of the peptide, n the number of residues, L the optical path in centimeters, ΔA the difference of absorption between left and right polarization, and c the peptide concentration in milligrams per milliliter.

2.5. Small-Angle X-ray Scattering. Small-angle X-ray scattering experiments were performed with a rotating anode (Rigaku, Japan, high brilliancy RU-200BEH), with a copper target and an effective source size of 0.1 × 0.1 mm^2. The anode operates at the voltage 40 kV and the current 25 mA. The Kα wavelength (1.54 Å) is selected by a quartz mirror covered with a gold layer. This mirror is curved in order to focus the beam and to eliminate the short wavelengths. A nickel filter eliminates the Kβ wavelength (1.39 Å). A gas detector (xenon/CO_2, Elphyse, France) with a window (3 mm × 50 mm) collects the signal: it has 512 channels (99 channels/cm). The resolution of the detector is 200 μm. The sample to detector distance is 825 mm. The dimension of the beam on the detector is 3 × 0.3 mm^2. The final resolution of the setup is 0.017 nm^{-1}. Samples were sealed in 1 mm diameter and 20 μm thick glass capillaries (Hilgenberg, Germany) and placed in a thermostated sample holder regulated with an accuracy of ±0.1 °C. The scattered intensity was corrected from the absorption of the sample. The background scattering of water (the most important solvent in volume) and glass was subtracted from the sample signal. To obtain the Caillé parameter η, the whole X-ray spectrum was fitted (except for very low q) using Nallet et al.'s[29] analytical approach based on Caillé's model,[30] where η is related to the elastic constants κ and $\bar{B}$ of the lamellar phase by the following expression:

$$\eta = {q_0}^2\frac{k_BT}{8\pi\sqrt{K\bar{B}}} \tag{2}$$

with $q_0 = 2\pi/d_B$ the position of the first-order quasi-Bragg singularity and $K = \kappa/d_B$, where d_B is the lamellar period. Since the electronic densities of water, the polar heads of the surfactant (ethylene glycol), and the peptide are very close (≈330 e·nm^{-3}), as well as the electronic densities of decane and the surfactant chains (≈260 e·nm^{-3}), we have chosen the following form factor for the lamella in Nallet et al.'s fit:

$$P(q) = \frac{2\Delta\rho^2}{q^2}\left[1 - \cos(qd_L)\exp\left(-\frac{q^2{d_L}^2}{32}\right)\right] \tag{3}$$

where d_L is the thickness of decane and surfactant chains.

To estimate the variation of the bilayer rigidity, κ, with the peptide concentration, the lamellar phase was studied along a dilution line: the bilayer thickness was kept constant [e.g. $V_s/(V_s + V_{decane}) = 0.55$] as well as the peptide concentration, while the periodicity was increased with water dilution. From geometrical considerations for stiff nonundulating bilayers, the bilayer thickness δ is related to the Bragg distance d_B and the bilayer volume fraction ϕ by

$$\phi = \frac{\delta}{d_B} \tag{4}$$

which is called the classical dilution law.[31] When the lamellar phase is stabilized by thermal fluctuations, the bilayers are fluctuating, so the projected area of a bilayer is smaller than the real area and the classical dilution law is not exactly valid anymore. For large bilayer volume fraction ϕ, the corrected dilution law becomes[32−34]

$$d_B\phi = V - W\ln(d_B - \delta) \tag{5}$$

with

$$W = \delta\frac{k_BT}{4\pi\kappa} \tag{6}$$

and

$$V = \delta\left(1 + \frac{k_BT}{4\pi}\ln\left[\sqrt{\frac{32\kappa}{3\pi k_BT}}\frac{1}{a}\right]\right) \tag{7}$$

where a is a molecular dimension. The approached value of δ is deduced from the classical dilution law and κ has been determined either by inserting the δ value into eq 5 or directly from the ratio V/W. Both methods give the same value with an accuracy of 10−15%.

2.6. Deuterium NMR. NMR measurements were performed on a Bruker DMX 400, wide bore spectrometer operating at 61.4 MHz for ^{2}H, using a 10 mm liquid probe. Spectra were acquired using a simple Bloch decay with no Hahn echo or proton decoupling. Typical acquisition parameters were as follows: 90° pulse length of 26 μs; a recycle delay of 1 ms; a spectral width of 10 kHz; and 256 scans for a total of 4 min per spectrum. 16K complex points were acquired, zero filled to 32K before Fourier transformation with 1 Hz exponential line broadening and automatic baseline correction. All samples were maintained at 20 °C by air circulation.

Recently, Auguste et al.[35] have used NMR to measure the rigidity of a lamellar phase bilayer. The typical quadrupolar splitting, $\Delta\nu_Q$, of a lamellar phase depends of the rigidity, κ, as follows:

$$\Delta\nu_Q = A\left[\frac{3}{1 + \frac{k_BT}{8\pi\kappa}\ln\left[1 + \frac{\kappa d_B(\pi/a)^4}{\bar{B}}\right]} - 1\right] \tag{8}$$

where A is a constant and $\bar{B}$ the smectic compressibility modulus. In the case of a lamellar phase stabilized by thermal fluctuations, $\bar{B}$ can be replaced by the expression[36]

$$\bar{B} = d_B\frac{9\pi^2(k_BT)^2}{64\kappa {d_w}^4} \tag{9}$$

where d_w is the water thickness. $\Delta\nu_Q$ then becomes

$$\Delta\nu_Q = A\left[\frac{3}{1 + \frac{k_BT}{8\pi\kappa}\ln\left[1 + \frac{64\kappa^2 {d_w}^4(\pi/a)^4}{9\pi^2(k_BT)^2}\right]} - 1\right] \tag{10}$$

The more rigid the bilayer, the smaller the quadrupolar splitting. In our experiments, the organic solvent was deuterated: half by weight of the decane in the sample was replaced by perdeuterated decane. In that case, $\Delta\nu_Q$ was further reduced by the local dynamics of decane, if any.

(29) Nallet, F.; Laversanne, R.; Roux, D. *J. Phys. II* **1993**, *3*, 487.
(30) Caillé, A. *C. R. Hebd. Acad. Sci. Paris B* **1972**, *274*, 891.
(31) Larche, F. C.; El Qebbaj, S.; Marignan, J. *J. Phys. Chem.* **1986**, *90*, 707.
(32) Helfrich, W.; Servuss, R. M. *Il Nuovo Cimento* **1984**, *3*, 137.
(33) Golubovic, L.; Lubensky, T. C. *Phys. Rev. B* **1989**, *39*, 12110.
(34) Roux, D.; Nallet, F.; Freyssingeas, E.; Porte, G.; Bassereau, P.; Skouri, M.; Marignan, J. *Europhys. Lett.* **1992**, *17*, 575.
(35) Auguste, F.; Barois, P.; Fredon, L.; Clin, B.; Dufourc, E. J.; Bellocq, A.-M. *J. Phys. II* **1994**, *4*, 2197.
(36) Safinya, C. R.; Roux, D.; Smith, G. S.; Sinha, S. K.; Dimon, P.; Clarck, N. A.; Bellocq, A.-M. *Phys. Rev. Lett.* **1986**, *57*, 2718.

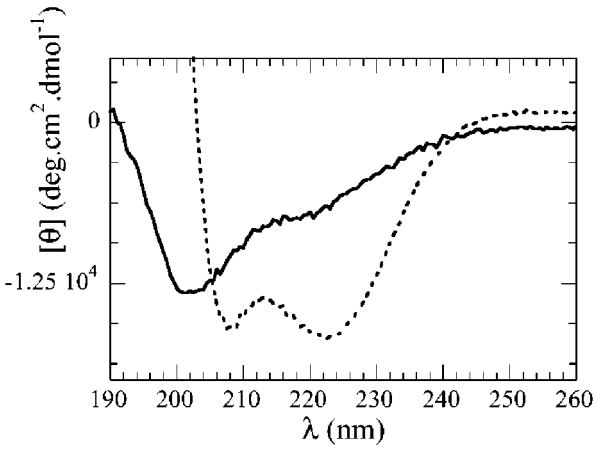

Figure 1. Circular dichroism spectra of the peptide in aqueous solution ($c = 0.83$ mg/mL, solid line) and in the sponge phase ($c = 0.515$ mg/mL, dotted line) at 28 °C. The first spectrum is characteristic of an unordered peptide, whereas the second, with the double minimum at 208 and 222 nm, is characteristic of an α-helix. The presence of surfactant bilayers enhances the organization. According to the method of Chen et al.,[37] the percentage of the peptide in the in α-helical conformation is 40%, corresponding to 12 residues.

3. Results

3.1. Circular Dichroism. The far UV spectrum of the peptide in aqueous solution is presented in Figure 1. The shape of the curve is typical of an unordered molecule.[37] The far UV spectrum in the sponge phase (Figure 1), with its two minima at 208 and 222 nm, is characteristic of an α-helix.[37] Obviously, the presence of bilayers enhances the peptide organization. As expected from the modeling, a part of the peptide is organized into an α-helix. Using the empirical formula of Chen et al.,[37] the percentage of α-helix has been evaluated:

$$\%\ \alpha\text{-helix} = \frac{[\theta]}{395}\left(\frac{2.57}{n-1} - 1\right) \qquad (11)$$

where $[\theta]$ is the mean residue ellipticity at 222 nm and n is the number of residues in the peptide. One finds that 40% of the peptide is α-helical in the sponge phase, which corresponds to 12 residues. The structured hydrophilic part is then 1.8 nm long (12 residues × 0.15 nm rise per residue[38]).

3.2. Surface Tension Measurements. To check if the peptide is located at the hydrophilic−hydrophobic interface, surface tension measurements have been carried out at the water−decane interface. In the absence of peptide, the water−decane surface tension measured is equal to 48 mN/m. This result is in relatively good agreement with the value $\gamma_{w-d} = 53 \pm 2$ mN/m measured by Goebel and Lunkenheimer.[39] When a small amount of peptide (0.105 mg/mL) is dissolved in aqueous solution, the surface tension decreases to 30mN/m, indicating that the peptide is located at the water−decane interface because of its amphipathic structure.

3.3. Spectrofluorometry. The peptide location is further confirmed by spectrofluorometry. In water, when excited at 280 nm, the peptide fluorescence presents a broad peak around 350 nm, which originates from the tryptophans (Trp's) (Figure 2). When the peptide is solubilized in the sponge phase, this peak is shifted (Figure 2) toward shorter wavelengths (340 nm). This shift means that the two Trp residues of the peptide sequence are in a more hydrophobic environment than that in aqueous solution. Together with surface tension measurements, these results confirm the nature of the environment: the peptide is at the hydrophobic−hydrophilic interface.

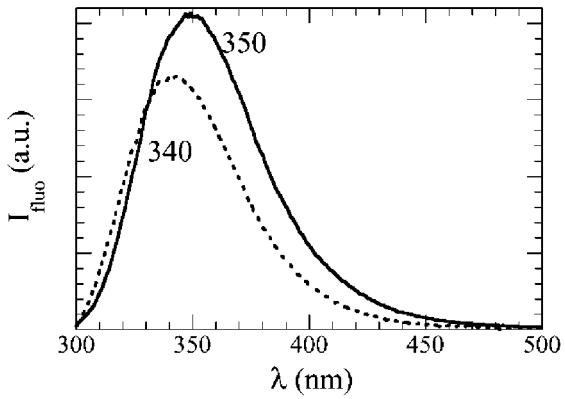

Figure 2. Fluorescence spectra of the peptide in aqueous solution (plain line) and in the sponge phase (dotted line) performed at 28 °C. The peptide concentration is 0.035 mg/mL in both experiments. The excitation wavelength is 290 nm. The shift of the broad fluorescence peak of the tryptophan from 350 to 340 nm indicates a more hydrophobic environment for the peptide in the sponge phase.

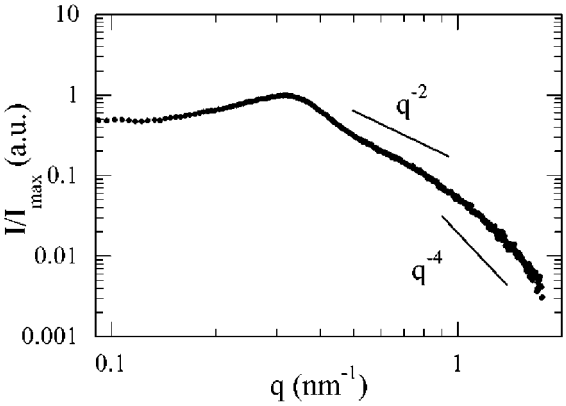

Figure 3. Typical SAXS spectrum of a sponge phase, in the log−log representation, with a correlation bump at q_1 and a dependence on q^{-2} and q^{-4} for $q > q_1$. This spectrum corresponds to the bilayer volume fraction $\phi = 0.38$ at 28 °C, for the ratio $V_s/(V_s + V_{decane}) = 0.55$.

3.4. Small-Angle X-ray Scattering. At 28 °C, to ascertain whether the system was in the relatively narrow L_3 phase domain, SAXS was carried out. In all cases, in the presence or the absence of peptide, our samples were isotropic. The spectra present a correlation bump at q_1, and the scattered intensity shows a dependence on q^{-2} and q^{-4} for $q > q_1$, typical elements of a sponge phase[40] (Figure 3).

The X-ray spectra of two lamellar phases are presented in Figure 4. When the peptide is added, the position of the quasi-Bragg peak remains constant: $q_0 = 0.42 \pm 0.005$ nm^{-1}, whereas the width of the peak decreases. The quasi-Bragg peak being constant tells us more about the orientation of the peptide relative to the bilayer: The hydrophobicity of the ending blocks of the peptide does

(37) Chen, Y.-H.; Yang, J. T.; Chau, K. H. *Biochemistry* **1974**, *13*, 3350.
(38) Setlow, R. B.; Pollard, E. C. *Molecular Biophysics*; Addison-Wesley: Reading, MA, 1962.
(39) Goebel, A.; Lunkenheimer, K. *Langmuir* **1997**, *13*, 369.
(40) Gazeau, D.; Bellocq, A.-M.; Roux, D.; Zemb, T. *Europhys. Lett.* **1989**, *9*, 447. Skouri, M.; Marignan, J.; Appel, J.; Porte, G. *J. Phys. II* **1991**, *1*, 1121. Schmidt, C. F.; Svoboda, K.; Ning Lei; Petsche, I.; Berman, L.; Safinya, C. R.; Grest, G. *Science* **1993**, *259*, 952.

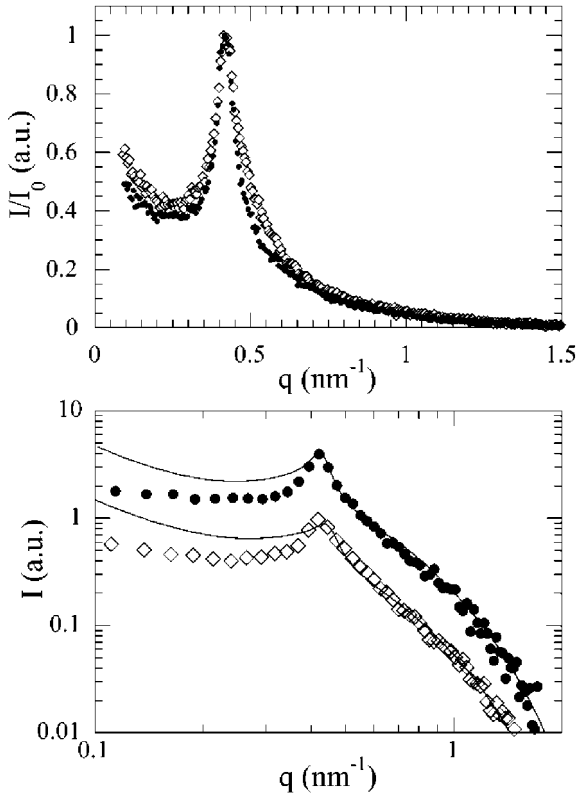

Figure 4. SAXS spectra of a "bare" lamellar phase ($R = 0$; ◇) and a peptide-decorated lamellar phase ($R = 5.2 \times 10^{-4}$; ●) in linear representation (top) and log−log representation (bottom). Only one point out of five has been presented on the bottom graph to enable the reader to distinguish the fit. Lines are the best fits according to the Nallet et al. analytical model.[28] The bilayer volume fraction is $\phi = 0.38$ in both cases. The position of the quasi-Bragg peak remains constant at $q_0 = 0.42 \pm 0.005$ nm^{-1}, whereas the peak sharpens with peptide concentration. The fwhm of the "bare" lamellar phase is around 0.16 nm^{-1} whereas it decreases around 0.11 nm^{-1} for the peptide-decorated phase (top).

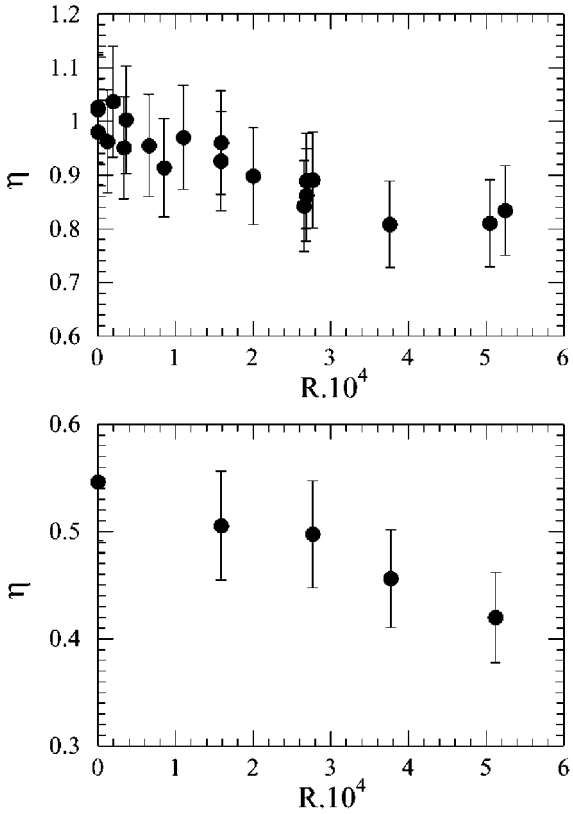

Figure 5. Variation of the Caillé parameter, η, obtained from the Nallet's fit of SAXS spectra versus the mole ratio of peptide to surfactant R ($\phi = 0.38$, top; $\phi = 0.48$, bottom).

not allow them to be soluble in water. Their exact configuration (inserted or adsorbed) is impossible to determine precisely; however, because no change in the quasi-Bragg peak has been observed, we can tell that the peptide does not pinch two opposite bilayers together as had been observed in other works.[24] Thus, the peptide must be lying on the bilayer surface.

The FWHM (full width at half maximum) of the "bare" lamellar phase is around 0.16 nm^{-1} whereas it decreases to around 0.11 nm^{-1} for the peptide-decorated phase (Figure 4, top). The sharpening of the peak is quantified by the Caillé parameter, η. The variation of η with R, the molar ratio of peptide to surfactant, is shown in Figure 5 (top): η decreases as the peptide concentration on the bilayer increases. This decrease is analogous to what has been observed when small concentrations of flexible end-grafted polymers are inserted into L_α phases.[18,19] The variation of η versus R for another bilayer volume fraction ($\phi = 0.48$) presents the same behavior (Figure 5, bottom).

3.5. Deuterium NMR. Figure 6 represents the typical spectra we obtain: for a "bare" lamellar phase ($R = 0$) and for a peptide-decorated lamellar phase ($R = 0.7 \times 10^{-4}$). Three quadrupolar splittings are present. The most intense (the central one) corresponds to the terminal CD_3 bound in decane, which has the maximum freedom. The two others can be associated to the CD_2 groups of the decane molecule. Usually all the splittings are sensitive to dilution; however, because of the bad insertion of decane

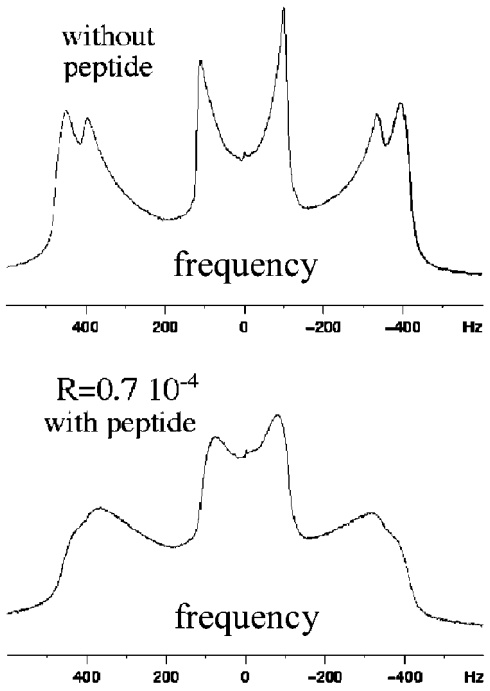

Figure 6. Deuterium NMR spectra of a "bare" lamellar phase ($R = 0$; top) and a peptide-decorated lamellar phase ($R = 0.7 \times 10^{-4}$; bottom) corresponding to the bilayer volume fraction $\phi = 0.52$. Both spectra exhibit three quadrupolar splittings as well as an isotropic peak. The splitting value decreases when peptides decorate the lamellar phase, which corresponds to a rigidification of the bilayer.

in the surfactant monolayer, the peaks are not all well resolved and we are only able to measure the variation of the central splitting. There is also a small isotropic

peak corresponding to deuterium molecules naturally present in water. The splitting was determined by measuring the peak positions with a ruler. This is justified when the lines are not too broad and when they are isolated.[41,42] The experimental resolution, as given by the ±20 Hz error, around the central peak allows such measurement and does not require spectral simulation. Such approximation could not be done on the other splittings, which is why they have been left aside. The quadrupolar splitting, $\Delta\nu_Q$, decreases when the peptide decorates the L_α phase: for $\phi = 0.52$, the more central $\Delta\nu_Q$ is 200 ± 20 Hz for the bare lamellar phase, whereas it decreases to 150 ± 20 Hz for the peptide-decorated phase. As the peptide-decorated phase is diluted, the difference between splittings becomes difficult to distinguish.

4. Discussion

We have checked that the sharpening of the quasi-Bragg peak did not originate from a residual electrostatic effect induced by the peptide. η remains the same whether the peptide-containing L_α phase is prepared with pure water or with brine (0.2 M NaCl), which screens electrostatic interactions: the peptide-decorated lamellar phase is still stabilized by thermal fluctuations, as is the "bare" one.

We have also checked that the width of the peaks was the same on a Bonse-Hart high resolution setup and on our device; therefore, we are sure that the η determination is correct with an accuracy of 10% (due to the choice of the limits of the fit or the starting parameters).

Since our samples are made of monolayers of surfactant alternatively separated by water and decane, one should consider[43] that

$$\bar{B} = \frac{\bar{B}_w \bar{B}_d}{\bar{B}_w + \bar{B}_d} \tag{12}$$

where $\bar{B}_w$ is given by expression 9 and $\bar{B}_d$ by expression 9 in which d_w is replaced by the decane thickness, d_d. The smectic compressibility modulus can be written as

$$\bar{B} = \bar{B}_w \left(1 + \left[\frac{d_d}{d_w}\right]^4\right)^{-1} \tag{13}$$

As soon as $d_d/d_w \ll 1$, $\bar{B} \approx \bar{B}_w$. The decane thickness, d_d, can easily be estimated by subtracting the thickness of the dry bilayer, δ_{dry} (without decane), from the bilayer thickness, δ. δ_{dry} can be determined by plotting d_B versus $1/\phi_s$ for high ϕ_s (volume fraction of surfactant) values:[44] it leads to $\delta_{dry} = 3.2$ nm (not shown). Thus, the decane thickness, $d_d = \delta - \delta_{dry} = 5.6 - 3.2 = 2.4$ nm. As 5.2 nm $\leq d_w \leq$ 9.4 nm, we finally obtain $0.25 = d_d/d_w = 0.5$ and $0.004 = [d_d/d_w]^4 = 0.0625$. The condition $d_d/d_w \ll 1$ is fulfilled, and we could consider hereafter our smectic phase as a stack of almost incompressible decane swollen bilayers, separated by water.

4.1. Variation of the Bilayer Thickness with Peptide Concentration. Replacing $\bar{B}$ by expression 9 in Caillé expression 2 leads to

$$\eta = \alpha\left(1 - \frac{\delta}{d_B}\right)^2 \tag{14}$$

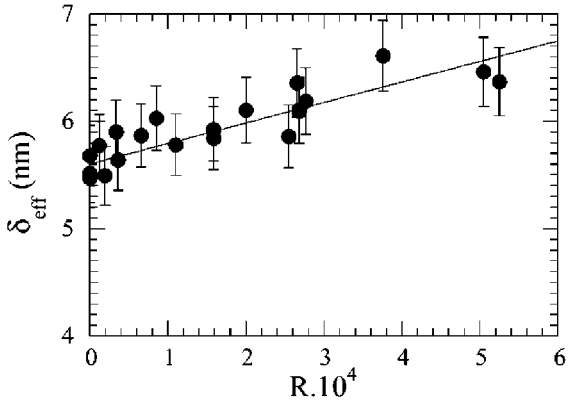

Figure 7. Variation of the effective bilayer thickness, δ_{eff}, obtained from $\delta_{eff}(R) = d_B[1 - (\eta(R)/\alpha)^{1/2}]$ versus the mole ratio of peptide to surfactant R ($\phi = 0.38$). We choose $\alpha = 2.5$ in order to obtain $\delta_{eff}(R = 0) = \delta_0 = 5.6$ nm. The best linear fit (line) gives $\delta_{eff}(R) = 5.6(1 + (0.34 \times 10^4)R)$ in nanometers.

where $\alpha = {}^4/_3$.[45] Experimental determination of α in real, nonidealized systems, however, can vary.[24] We would like to stress that the discrepancy could arise from the choice of the prefactor (which is far from settled) in expression 9: this prefactor varies from $9\pi^2/64 = 1.38$ according to Helfrich[46] to 0.638 according to Gomper and Kroll.[47] Choosing the Gomper and Kroll prefactor instead of Helfrich's leads us to replace $\alpha = {}^4/_3$ by $\alpha \sim 2$, not so far from 2.5 (see below).

Since in the present system, d_B is independent of peptide concentration, the decrease of η can be understood, according to Castro-Roman et al.,[19] by considering a renormalized bilayer thickness. From the previous expression for η, one has

$$\delta_{eff}(R) = d_B\left(1 - \sqrt{\frac{\eta(R)}{\alpha}}\right) \tag{15}$$

To find $\delta_{eff}(R = 0) = \delta_0 = 5.6$ nm, in agreement with the dilution law determination of the bilayer thickness, we have chosen α equal to 2.5. The effective bilayer thickness is found to increase linearly with R from 5.6 to 6.3 nm (Figure 7). This increase was not observed with SAXS experiments, because of the poor contrast between water and peptide electron densities. According to Aranda-Espinoza et al.,[48] the membrane perturbation induced by a rigid inclusion can lead to oscillations of the membrane thickness: locally the thickness of the membrane can be larger than the thickness of the inclusion. A crude geometrical model has been developed, with peptides decorating both sides of the bilayer (Figure 8). The arithmetic average of the bilayer thickness can thus be written as

$$\delta_{eff} = \delta_0 + 2\Delta h \phi_p \tag{16}$$

where Δh is the diameter of the peptide α-helix ($\Delta h = 1$ nm[38]) and ϕ_p the area fraction of bilayer perturbed by the peptide. This model can be considered as a crude average of the above-mentioned oscillations. The relationship between R and ϕ_p is

(41) Lafleur, M.; Fine, B.; Sternin, E.; Cullis, P. R.; Bloom, M. *Biophys. J.* **1989**, *56*, 1037−1041.
(42) Bouglet, G.; Ligoure, C.; Bellocq, A. M.; Dufourc, E.; Mosser, G. *Phys. Rev. E* **1998**, *57*, 834−842.
(43) Oda, R.; Litster, J. D. *J. Phys. II* **1997**, *7*, 815.
(44) Rajagopalan, V.; et al. *Langmuir* **1996**, *12*, 2939.
(45) Roux, D.; Safinya, C. R. *J. Phys. (Paris)* **1998**, *49*, 307.
(46) Helfrich, W. *Z. Naturforsch.* **1978**, *33a*, 305.
(47) Gompper, G.; Kroll, D. M. *Europhys. Lett.* **1989**, *9*, 59.
(48) Aranda-Espinoza, H.; Berman, A.; Dan, N.; Pincus, P.; Safran, S. *Biophys. J.* **1996**, *71*, 648−656.

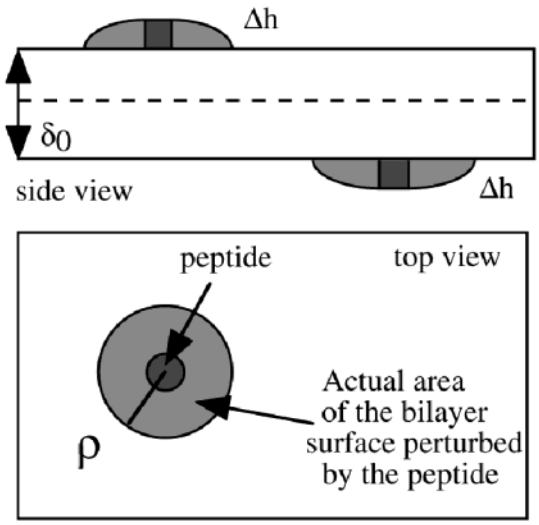

Figure 8. Schematic geometrical model of a bilayer decorated on both sides by peptides. Δh is the thickness of the peptide and ρ the radius of the zone where the peptide perturbs the bilayer.

$$\phi_p = R\frac{\Sigma}{\sigma} \tag{17}$$

with Σ the area perturbed by one peptide and σ the area per polar head of surfactant ($\sigma = 0.54$ nm^2[25]). The fit of δ_{eff} versus R allows one to estimate Σ to be 513 nm^2: the peptide affects the bilayer within a radius of $\rho = (\Sigma/\pi)^{1/2} \sim 13$ nm, much larger than the 1.8 nm length of the α-helix. The exact conformation of the hydrophobic regions of the peptide is not known. Even if we add an average of 0.1 nm per nonhelical residue, the overall length would be only 3.6 nm, which is still much smaller than the radius of perturbation induced by the peptide. However, this result is in qualitative agreement with the results of Dan et al.,[49] who predicted that a bilayer inclusion can perturb the bilayer within a radius equal to several times the inclusion size.

4.2. Variation of κ with Peptide Concentration. The bilayer bending rigidity κ was estimated from the correction to the dilution law. Two examples of the correction to the dilution law are presented in Figure 9, where the δ value taken in eqs 4−6 is the bare bilayer thickness ($\delta_0 = 5.6$ nm). The slope of the correction decreases as the peptide concentration increases: the peptide-decorated bilayers are more rigid than the bare ones. κ increases as the peptide decorates the lamellar phase. In Figure 10, the variation of κ with R is presented: κ increases 2-fold from $1k_BT$ for $R = 0$ to $2.2k_BT$ for $R = 5.2 \times 10^{-4}$. One can notice the large effect of the small peptide concentration. The rigidification is well fitted by a straight line: $\kappa = 0.8 + (0.25 \times 10^4)R$ in k_BT units (Figure 10).

The observed rigidification is qualitatively supported by the deuterium NMR data. The variation of $\Delta\nu_Q$ with the water thickness has been plotted in Figure 11. The $\Delta\nu_Q$ values corresponding to the bare lamellar phase are always more important than those for the peptide-decorated lamellar phase. But this variation of the quadrupolar splitting is difficult to fit because it is very small. Apparently, as a probe for bilayer rigidity, decane is less sensitive than a surfactant or a cosurfactant[35,42] because decane molecules experience local motion, as they are probably not located exactly at the hydrophobic−hydrophilic interface. Thus, a quantitative determination of κ is subject to caution, but the decrease of $\Delta\nu_Q$ is qualitatively in agreement with a rigidification of the lamellar phase induced by the peptide. The NMR experiments would be better with deuterated $C_{12}E_4$ instead of deuterated decane, but deuterated $C_{12}E_4$ is not a commercial product and is difficult to synthesize.

(49) Dan, N.; Pincus, P.; Safran, S. *Langmuir* **1993**, *9*, 2768.

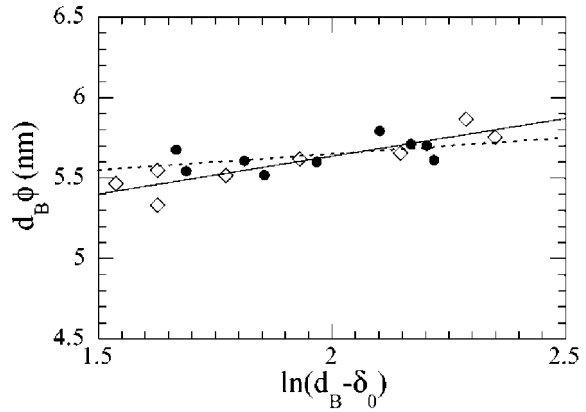

Figure 9. Corrections to the dilution law of a "bare" lamellar phase ($R = 0$; ◇) and a peptide-decorated lamellar phase ($R = 5.2 \times 10^{-4}$; ●), considering the effective thickness of the bilayer in eq 4. Lines are the best linear fits ($R = 0$, solid line; $R = 5.2 \times 10^{-4}$, dotted line). The decrease of the slope indicates that the peptide stiffens the bilayer.

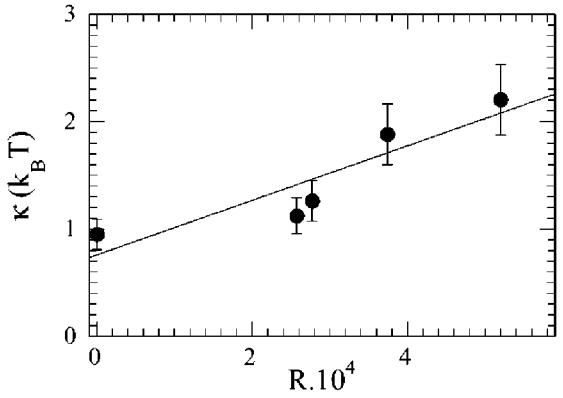

Figure 10. Variation of the bilayer bending rigidity, κ, versus the mole ratio of peptide to surfactant, R. The best linear fit (line) gives $\kappa = 0.8 + (0.25 \times 10^4)R$ (in k_BT units).

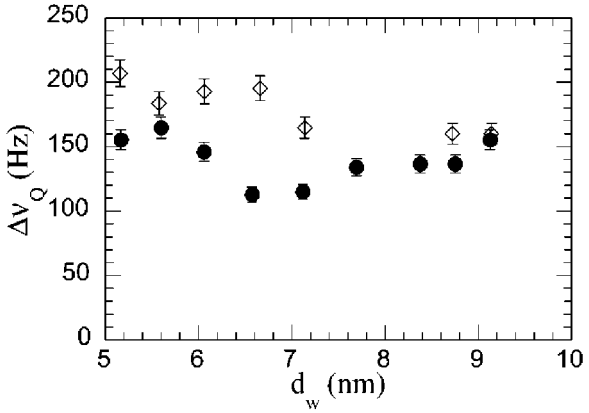

Figure 11. Variation of the quadrupolar splitting, $\Delta\nu_Q$, versus the water thickness, d_w, for a "bare" lamellar phase ($R = 0$; ◇) and a peptide-decorated lamellar phase ($R = 0.7 \times 10^{-4}$; ●). For the bare phase, $\Delta\nu_Q$ is always bigger than that for the peptide-decorated phase: this fact is qualitatively in agreement with a rigidification of the bilayer (see text). Because of the uncertainty and dispersion of the experimental points, a fit to expression 10 has not been performed.

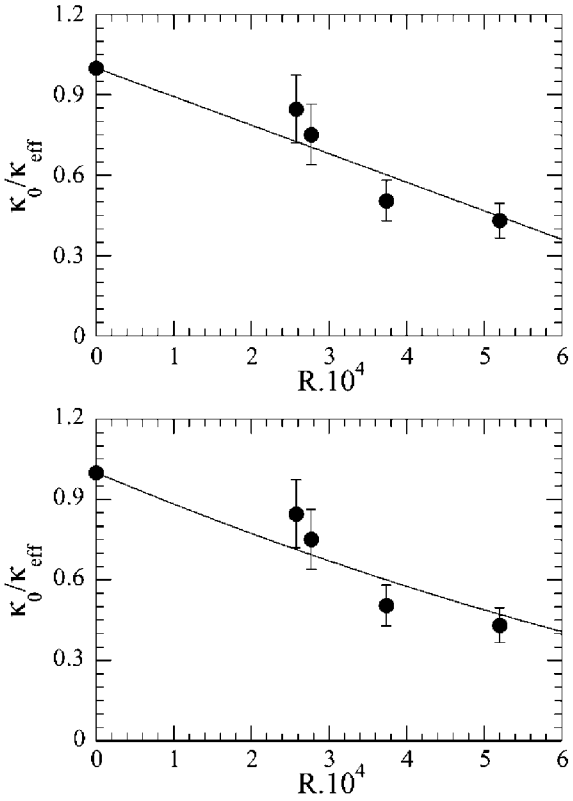

Figure 12. Variation of κ_0/κ_{eff} with the mole ratio of peptide to surfactant, R. The top graph corresponds to the best fit according to expression 18, whereas the bottom graph corresponds to the best fit according to expression 19 of the Netz−Pincus model. Both fits lead to inconsistent $\delta\kappa/\kappa_0$ values.

4.3. Comparison with Theoretical Models. To our knowledge, only three models exist for rigid inclusions. For an isolated bilayer, Netz and Pincus[21] have shown that the balance between attractive and repulsive interactions between inclusions leads to different types of inclusion distributions on the bilayer.

When inclusions are randomly dispersed and not aggregated (or organized) and the largest fluctuation wavelength is larger than the size of the surfactant:

$$\frac{1}{\kappa_{eff}} = \frac{1-\phi_i}{\kappa_0} + \frac{\phi_i}{\kappa_0 + \delta\kappa} \tag{18}$$

whereas if inclusions are aggregated, and if the size of the aggregates is larger than the largest fluctuation wavelength, the effective bilayer rigidity becomes

$$\frac{1}{\kappa_{eff}} = \left[\frac{1-\phi_i}{\sqrt{\kappa_0}} + \frac{\phi_i}{\sqrt{\kappa_0 + \delta\kappa}}\right]^2 \tag{19}$$

where $\delta\kappa$, the local increase of rigidity, originates from the inclusion, κ_{eff} is the effective rigidity of the bilayer, and ϕ_i is the surface fraction of inclusions on the bilayer. The above expressions are valid if $\delta\kappa/\kappa_0 \ll 1$. When fitted to the experimental values (Figure 12), replacing ϕ_i by $\phi_p = R\Sigma/\sigma$, the area fraction of bilayer perturbed by inclusions (eq 17), both expressions lead to inconsistent results: $\delta\kappa/\kappa_0 \approx -9.2$ for randomly dispersed (or organized) inclusions and $\delta\kappa/\kappa_0 \approx 6.5$ for aggregated inclusions. Thus, the Netz and Pincus model cannot account for the important rigidification induced by the peptide.

Chen considered a cylinder-coated lamellar phase:[22] he predicted that the rigidity should increase with cylinder concentration, whereas the lamellar period, d_B, and the bilayer thickness, δ, should decrease. In our system, the period remains constant and the effective bilayer thickness increases. Therefore, Chen's model cannot be applied to our results either.

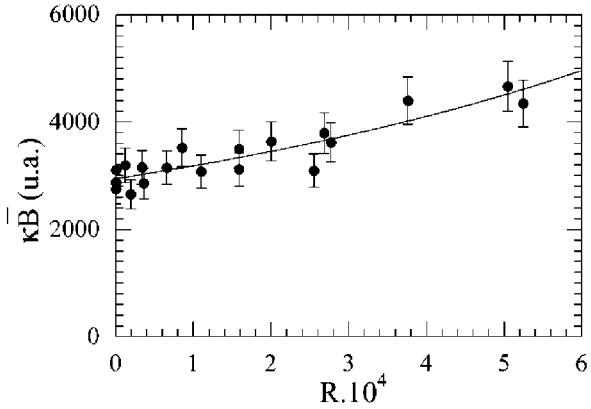

Figure 13. Variation of $\kappa\bar{B}$ with the mole ratio of peptide to surfactant, R. The curve corresponds to the best fit according expression 20 of the Sens−Turner model. It gives $\delta\kappa/\kappa_0 = 0.8 \pm 0.08$, within the limits of application of the model. The peptide presence induces a doubling of the local rigidity.

Sens and Turner[23] recently focused on the effect of three types of inclusions on the product of the elastic constants $K\bar{B}$ of a lamellar phase. The inclusion called "rigid" seems to correspond to our peptide because of the sharpening of the quasi-Bragg peak. If $(\delta\kappa/2\kappa_0)\phi_i \ll 1$, the effective $(K\bar{B})_{eff}$ can be written as

$$(K\bar{B})_{eff} = \frac{(K\bar{B})_0}{\left(1 - \frac{\delta\kappa}{2\kappa_0}\phi_i\right)^2} \tag{20}$$

where ϕ_i is the area fraction of inclusions on the bilayer. Our experimental results ($\kappa\bar{B}$ instead of $K\bar{B}$) have been fitted with expression 20 (Figure 13) taking $\phi_i = \phi_p$, the area fraction of bilayer perturbed by the peptide (expression 17). The fit is good and gives $(\kappa\bar{B})_0 = (2950 \pm 50)$ in k_BT·Pa units and $\delta\kappa/\kappa_0 = 0.8 \pm 0.08$. Concerning $\delta\kappa/\kappa_0$, since R varies between 0 and 5.2×10^{-4}, one finds $0 < \phi_p < 0.5$ and the condition $(\delta\kappa/2\kappa_0)\phi_i \ll 1$ is always fulfilled. According to the Sens−Turner model, the local increase of rigidity that originates from the peptide is roughly twice the rigidity of the bare bilayer. However, the effective rigidity of the bilayer cannot be deduced because of the simultaneous $\bar{B}$ variation as shown below.

Finally, from the independent determination of $\eta(R)$ and $\kappa(R)$, and Caillé's formula 2, the variation of $\bar{B}$ as a function of R has been deduced. $\bar{B}$ decreases with peptide concentration (Figure 14): the peptide insertion in the present system softens interactions between bilayers, whereas all experimental studies on flexible end-grafted polymers have observed the contrary.[18,20]

5. Conclusion

A neutral rigid triblock peptide (hydrophobic−hydrophilic−hydrophobic) has been synthesized. Circular dichroism experiments have shown that the peptide is unordered in aqueous solution, whereas its hydrophilic part becomes α-helical in the presence of bilayers of surfactant enclosing decane. Surface tension measurements as well as spectrofluorometry have proved that the peptide is at the hydrophilic−hydrophobic interface.

When inserted in small concentrations into a lamellar phase stabilized by thermal fluctuations, the peptide

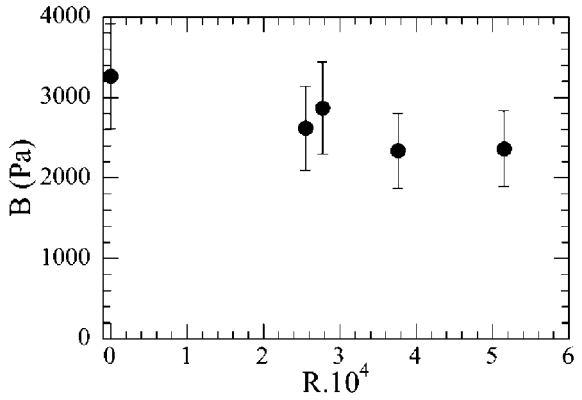

Figure 14. Experimental variation of the smectic compressibility modulus B versus the mole ratio of peptide to surfactant, R. The peptide presence leads to a softening of bilayer interactions.

induces a sharpening of the quasi-Bragg peak, whereas the periodicity of the lamellar phase remains unchanged. Together with surface tension measurements and spectrofluorometry, this last piece of data indicates that the peptide lies on the bilayer surface. The sharpening of the quasi-Bragg peak is not due to electrostatic interactions. The Caillé parameter, η, decreases with peptide concentration. Since the peptide decorated lamellar phase remains stabilized by thermal fluctuations, this decrease can be interpreted as an increase of the bilayer effective thickness. A simple geometrical model with peptides adsorbed on the bilayer explains this renormalization of the bilayer thickness and leads also to an estimate of 13 nm as the radius of the perturbation induced by the peptide. This extension can be qualitatively explained by the thickness mismatch between the peptide and the bilayer. Systematic measurements of variation of the bending rigidity show that small amounts of the peptide induce a dramatic stiffening of the lamellar phase. The bending rigidity of a bare bilayer increases 3-fold for mole ratios of peptide-to-surfactant as low as $R = 5.2 \times 10^{-4}$. Among published results for flexible end-grafted polymers,[18−20] only Yang et al.[20] observed a doubling of κ with concentration 30 times higher than our peptide concentration. As far as rigid transbilayer inclusions are concerned, no variation of κ was observed.[24] Our experimental results are well fitted by the Sens and Turner model. The spectacular rigidification of the bilayer arises from the local rigidity originating from the peptide: this local rigidity is roughly the double of the rigidity of the bare bilayer. The peptide also leads to a softening of interactions between decorated bilayers (e.g. decrease of $\bar{B}$).

Acknowledgment. The authors would like to thank J. Meunier for suggesting the surface tension experiments, E. Bertrand for his help with these measurements, E. Cogne for spectrofluorometry, and Y. K. Yip for the peptide synthesis. We also acknowledge valuable discussions with F. Pincet, C. Ligoure, F. Castro-Roman, P. Sens, and J. Meunier. N.T. was supported by a "Société de Secours des Amis des Sciences" fellowship. P.K. acknowledges the support of the New Jersey Agriculture Experiment Station (Paper D-01405-1-01).

LA015745C